Eur. Phys. J. A **13**, 405–410 (2002)
DOI 10.1140/epja/iepja1286

THE EUROPEAN
PHYSICAL JOURNAL A

Charged-particle multiplicity distributions in different rapidity windows in 800 GeV proton-nucleus interactions

Namrata, Ashutosh Bhardwaj, Kirti Ranjan, Sudeep Chatterji, Ajay K. Srivastava, V.K. Verma, and R.K. Shivpuri[a]

Centre for Detector and Related Software Technology, Department of Physics and Astrophysics, University of Delhi, Delhi-110 007, India

Received: 30 August 2001 / Revised version: 16 January 2002
Communicated by W. Henning

Abstract. Multiplicity distributions of charged particles produced in interactions of 800 GeV protons with emulsion nuclei in various rapidity windows are presented. The data is also analyzed separately for the forward and the backward hemispheres, for rapidity windows of different widths. It is found that the Negative Binomial Distribution (NBD) describes well the multiplicity distribution of secondary particles in various rapidity windows and also in both the hemispheres. We have compared the NBD parameters, in both the hemispheres, at 200 GeV and 360 GeV, with those at 800 GeV. The behaviour of NBD parameters in rapidity windows of different widths and for different targets has also been studied.

PACS. 13.85.-t Hadron-induced high- and super-high-energy interactions (energy > 10 GeV) – 13.85.Hd Inelastic scattering: many-particle final states

1 Introduction

In recent years, the study of Multiplicity Distributions (MDs) in high-energy interactions has revealed that charged-particle MDs have a Negative Binomial (NB) shape over a wide energy range in full phase space. A variety of collisions such as hadronic, hadron-nucleus, nucleus-nucleus, leptonic and semi-leptonic (see *e.g.* [1–15] and references therein) are well described by Negative Binomial Distribution (NBD). It has attained the status of a new empirical law. NBD is of the form [16]

$$P(n) = \frac{k(k+1)...(n+k+1) \quad \overline{n}^n \; k^k}{n!(\overline{n}+k)^{n+k}}\,, \qquad (1)$$

where, $P(n)$ is the probability of finding n charged particles in the final state, $\overline{n}$ is the average multiplicity and k is related to dispersion D by

$$\frac{D^2}{\overline{n}^2} = \frac{1}{\overline{n}} + \frac{1}{k}\,. \qquad (2)$$

The parameter $1/k$ is considered as a measure of aggregation of particles into clans and is given by

$$\frac{1}{k} = \frac{P_1(2)}{P_2(2)}\,,$$

i.e., it corresponds to the ratio of the probability to have two particles in the same clan, $P_1(2)$, to the probability to have the two particles into two separate clans, $P_2(2)$. So, in effect, k governs the width of the distribution. Also, in more general terms, k is linked to the two-particle correlation function $C_2(y_1, y_2)$ and to the second-order factorial cumulant, κ_2, by the equation

$$\frac{1}{k} = \kappa_2 = \int C_2(y_1, y_2)\mathrm{d}y_1\mathrm{d}y_2\,.$$

Various theoretical attempts have been made to obtain a NBD law from general principles but the most widely used approach is the clan model [17,18]. Negative binomial distribution can be produced by a two-step process. In the first step, the clans are distributed as a Poisson distribution and in the second step, each clan decays into final particles independently, with logarithmic distribution. Hence, overall multiplicity distribution is of NB form.

The clan parameters, namely, the average clan multiplicity $\overline{N}$ and average clan size $\overline{n_\mathrm{c}}$ are related to NBD parameters, *i.e.*, $\overline{n}$ and k by

$$\begin{aligned} \overline{N} &= k \; \ln[1 + \overline{n}/k]\,, \\ \overline{n_\mathrm{c}} &= \overline{n}/\overline{N}\,. \end{aligned} \qquad (3)$$

The clan model is meaningful for $1/k > 0$, ($\overline{N} \ll n$, $\overline{n_\mathrm{c}} \geq 1$), *i.e.*, for the genuine NBD. The value of $1/k$ is a measure of the particle aggregation ($1/k = 0$ for $\overline{n_\mathrm{c}} = 1$).

At parton level, clan formation can be explained by Generalized Simplified Parton Shower (GSPS) model [19]. In this model, energy-momentum conservation laws are

[a] e-mail: hep@nda.vsnl.net.in

relaxed locally, but are maintained at the global level, according to the physical existence of the clans [20]. Clans are considered as independent active parton sources, the average number of clans in each event coinciding with the number of steps of the cascade originating from an initial parton, *i.e.*, with the number of splittings of the ancestor (an ancestor splits n times, giving rise to n sub-processes, one sub-process at each split, and these are identified with the clans). The generation of clans is independent of the previous history, and hence, the process is Markoffian. The simple physical picture of the parton level presented above can be carried over to the hadronic level by Generalized Local Parton-Hadron Duality (GLPHD) [21]. It was proposed on the basis of the approximate occurrence of NBD both at the final parton level in Monte Carlo simulations and at the final hadron level.

The wide application of NBD has prompted us to check its validity in proton-nucleus interactions at 800 GeV, which is the highest available energy for fixed targets. One of us (RKS) had shown earlier [22] that NBD fits the multiplicity distribution well over the entire phase space. In this paper, we try to fit NBD in limited rapidity windows and also, for different target masses. We find that NBD fits well for each of the rapidity windows and also for each target. We have also analyzed the variation of $\overline{n}$, $1/k$, $\overline{N}$ and $\overline{n_c}$ with change in width of $\Delta\eta$, and also with change in primary energy. We find that these parameters show similar behavior for different primary energies, different targets, and different rapidity windows, *i.e.*, they are like "universal" parameters. It would be interesting to see if such a behaviour of NBD parameters would be exhibited at LHC energies.

2 Experimental details

A stack of 40 Ilford G5 emulsion pellicles of dimensions $10 \times 8 \times 0.06$ cm^3 was exposed to a proton beam of energy 800 GeV at Fermilab. The beam flux was 8.7×10^4 particles/cm^2. The scanning of the interactions was done under 40× objective of the high-resolution microscopes by the area scanning method. The scanning efficiency, for each observer, was calculated using the double-scan data and the overall efficiency was found to be 99%. All the interactions were followed back, in order to ensure that they are due to beam tracks only. The interactions lying within 25 μm each from the air and glass surface have not been considered for measurement. Taking these criteria into account, the total number of primary interactions was found to be 3390. All the measurements were done under 100× oil immersion objective. Following the usual emulsion terminology, the secondary particles having ionisation $I \leq 1.4I_0$ and $I > 1.4I_0$ were designated as shower ($N_{\rm s}$) and heavy tracks ($N_{\rm h}$), respectively, where I_0 is the ionization of the primary particle. The space angle (θ) and the azimuthal angle (ϕ) of the shower tracks with respect to beam tracks were measured by the co-ordinate method. The values of x, y and z co-ordinates at the vertex and two points each on the shower and beam tracks were measured, and their angles were determined. The uncertainty in angle measurement was 8×10^{-4} radians. Pseudorapidity (η) of shower particles is given by

$$\eta = -\ln[\tan(\theta/2)],$$

and it is a good approximation to rapidity for very high energies. It has been shown [23] that the target nucleus can be broadly identified on the basis of value of $N_{\rm h}$, as $N_{\rm h}$ reflects the number of nucleons of the target nucleus that have participated in the interaction. The interactions having $N_{\rm h} \leq 1$, $2 \leq N_{\rm h} \leq 5$ and $N_{\rm h} \geq 9$ can be assumed to belong to nucleon, CNO and AgBr targets, respectively. The interactions with $N_{\rm h} \leq 1$ are either due to collision with pure H nuclei or due to the interactions with a single nucleon of other emulsion nuclei, wherein the rest of the nucleus remains a spectator during the collision. The shower particle production takes place only in the elementary proton-nucleon collision. The interactions with $2 \leq N_{\rm h} \leq 5$ were considered to belong mostly to proton-light nuclei (CNO) interactions. The interactions with $6 \leq N_{\rm h} \leq 8$ are not considered as they could be from collisions with light nuclei as well as with heavy nuclei. The interactions with $N_{\rm h} \geq 9$ are unambiguous interactions with AgBr nuclei. In the present work, the total number of interactions of the type proton-nucleon, proton-CNO and proton-AgBr are found to be 615, 908 and 1388, respectively.

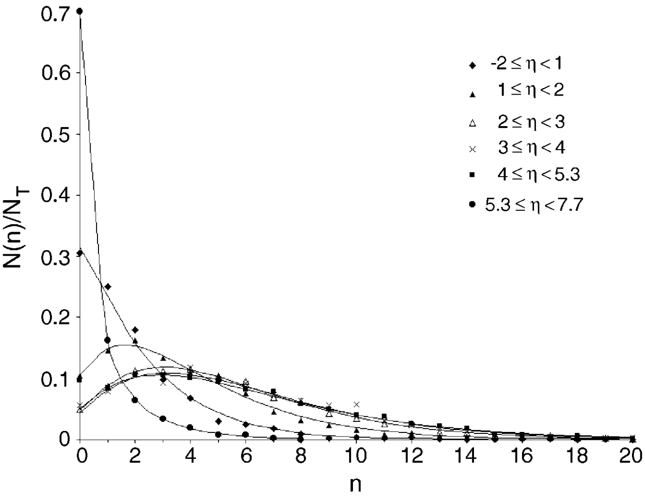

Fig. 1. Normalized multiplicity distribution, ($N(n)/N_{\rm T}$, where $N(n)$ is the number of shower particles in n-th bin and $N_{\rm T}$ is the total number of events) for different rapidity windows: a) $-2.0 \leq \eta < 1.0$, b) $1.0 \leq \eta < 2.0$, c) $2.0 \leq \eta < 3.0$, d) $3.0 \leq \eta < 4.0$, e) $4.0 \leq \eta < 5.3$, f) $5.3 \leq \eta < 7.7$. Only the p-AgBr interactions are shown for clarity.

3 Results and discussion

The predictions of NB distributions have been fitted to the observed multiplicity distribution for proton-nucleon (p-N) and proton-nucleus interactions at 800 GeV for different rapidity windows. The average multiplicity from experiment is taken to be the input for fitting the NBD to

Table 1. Values of average multiplicity ($\overline{n}$), k, average clan multiplicity ($\overline{N}$) and average clan size ($\overline{n_c}$) for different rapidity windows and different targets.

Rapidity windows		k	$\overline{n}$	$\overline{N}$	$\overline{n_c}$
$-2.0 \le \eta < 1.0$	N_h-all	0.63 ± 0.01	1.11 ± 0.02	0.6 ± 0.01	1.7 ± 0.03
	$N_h \le 1$	0.41 ± 0.02	0.31 ± 0.01	0.2 ± 0.01	1.3 ± 0.05
	$2 \le N_h \le 5$	0.51 ± 0.02	0.69 ± 0.02	0.4 ± 0.01	1.6 ± 0.05
	$N_h \ge 9$	1.20 ± 0.03	1.94 ± 0.05	1.2 ± 0.03	1.7 ± 0.05
$1.0 \le \eta < 2.0$	N_h-all	1.28 ± 0.02	2.47 ± 0.05	1.4 ± 0.02	1.8 ± 0.03
	$N_h \le 1$	1.62 ± 0.07	0.92 ± 0.04	0.7 ± 0.03	1.3 ± 0.05
	$2 \le N_h \le 5$	1.95 ± 0.06	1.58 ± 0.05	1.2 ± 0.02	1.4 ± 0.02
	$N_h \ge 9$	2.22 ± 0.06	3.89 ± 0.22	2.2 ± 0.06	1.7 ± 0.05
$2.0 \le \eta < 3.0$	N_h-all	1.80 ± 0.03	3.91 ± 0.07	2.1 ± 0.04	1.9 ± 0.04
	$N_h \le 1$	1.26 ± 0.05	2.18 ± 0.09	1.3 ± 0.05	1.7 ± 0.07
	$2 \le N_h \le 5$	2.05 ± 0.07	2.99 ± 0.22	1.8 ± 0.03	1.6 ± 0.03
	$N_h \ge 9$	2.81 ± 0.07	5.46 ± 0.15	3.0 ± 0.08	1.8 ± 0.05
$3.0 \le \eta < 4.0$	N_h-all	2.15 ± 0.04	4.74 ± 0.08	2.5 ± 0.04	1.9 ± 0.03
	$N_h \le 1$	1.95 ± 0.08	3.27 ± 0.13	1.9 ± 0.08	1.7 ± 0.07
	$2 \le N_h \le 5$	2.12 ± 0.07	3.98 ± 0.13	2.2 ± 0.07	1.8 ± 0.06
	$N_h \ge 9$	2.63 ± 0.07	5.98 ± 0.16	3.1 ± 0.08	1.9 ± 0.05
$4.0 \le \eta < 5.3$	N_h-all	3.11 ± 0.05	5.10 ± 0.09	3.0 ± 0.05	1.7 ± 0.03
	$N_h \le 1$	5.00 ± 0.20	5.11 ± 0.21	3.5 ± 0.4	1.5 ± 0.06
	$2 \le N_h \le 5$	3.50 ± 0.12	5.38 ± 0.18	3.3 ± 0.11	1.7 ± 0.05
	$N_h \ge 9$	2.29 ± 0.06	6.11 ± 0.16	3.0 ± 0.08	2.1 ± 0.06
$5.3 \le \eta < 7.7$	N_h-all	0.41 ± 0.01	0.82 ± 0.02	0.5 ± 0.01	1.8 ± 0.03
	$N_h \le 1$	0.52 ± 0.02	1.05 ± 0.04	0.6 ± 0.01	1.8 ± 0.03
	$2 \le N_h \le 5$	0.48 ± 0.02	0.93 ± 0.03	0.5 ± 0.02	1.8 ± 0.06
	$N_h \ge 9$	0.37 ± 0.01	0.61 ± 0.02	0.4 ± 0.01	1.7 ± 0.04

Table 2. Values of average multiplicity ($\overline{n}$), $1/k$, average clan multiplicity ($\overline{N}$) and average clan size ($\overline{n_c}$) for p-nucleus interactions at different primary energies.

Primary energy (GeV)	Interaction type	F/B region	Average multiplicity ($\overline{n}$)	$1/k$	Average clan multiplicity ($\overline{N}$)	Average clan size ($\overline{n_c}$)	Ref.
200	p-Xe	F	5.78 ± 0.22	0.077 ± 0.014	4.78 ± 0.16	1.21 ± 0.04	[3]
		B	14.00 ± 0.53	0.648 ± 0.038	3.57 ± 0.13	3.93 ± 0.18	
200	p-Ar	F	5.26 ± 0.14	0.122 ± 0.024	4.15 ± 0.21	1.27 ± 0.05	[3]
		B	9.22 ± 0.40	0.487 ± 0.047	3.50 ± 0.17	2.64 ± 0.16	
360	p-Al	F	6.55 ± 0.70	0.250 ± 0.120	3.87 ± 0.41	1.69 ± 0.18	[24]
		B	12.68 ± 2.33	0.640 ± 0.200	3.45 ± 0.63	3.67 ± 0.67	
360	p-Au	F	7.14 ± 0.31	0.150 ± 0.050	4.85 ± 0.21	1.47 ± 0.06	[24]
		B	19.17 ± 0.99	0.620 ± 0.070	4.12 ± 0.21	4.65 ± 0.24	
800	p-emulsion	F	9.22 ± 0.16	0.480 ± 0.009	3.52 ± 0.06	2.62 ± 0.05	Present work
		B	11.79 ± 0.20	0.498 ± 0.009	3.87 ± 0.07	3.04 ± 0.05	

the data and the value of k is obtained by the CERN computer program MINUIT.

We have studied here the MDs for p-N, p-CNO, and p-AgBr interactions separately. The rapidity windows that we have chosen are in the backward region ($-2.0 \le \eta < 1.0$ and $1.0 \le \eta < 2.0$), central region ($2.0 \le \eta < 3.0$, $3.0 \le \eta < 4.0$ and $4.0 \le \eta < 5.3$) and forward region ($5.3 \le \eta < 7.7$).

Figure 1 shows the experimental multiplicity distribution for different rapidity windows. The solid line gives the NBD fit to experimental values. For brevity, only the MDs for p-AgBr interactions have been shown. It can be seen that the NBD reproduces well the experimental values, in each of the rapidity windows. We obtained $\chi^2/\mathrm{DOF} < 1$ for all the distributions. Similar results were obtained for p-N and p-CNO interactions. This supports the proposition that NBD is a "universal" distribution, independent of the target mass, and rapidity window considered.

We have also calculated the clan parameters —k, $\overline{n}$, $\overline{N}$ and $\overline{n_c}$— for each of the rapidity windows for the con-

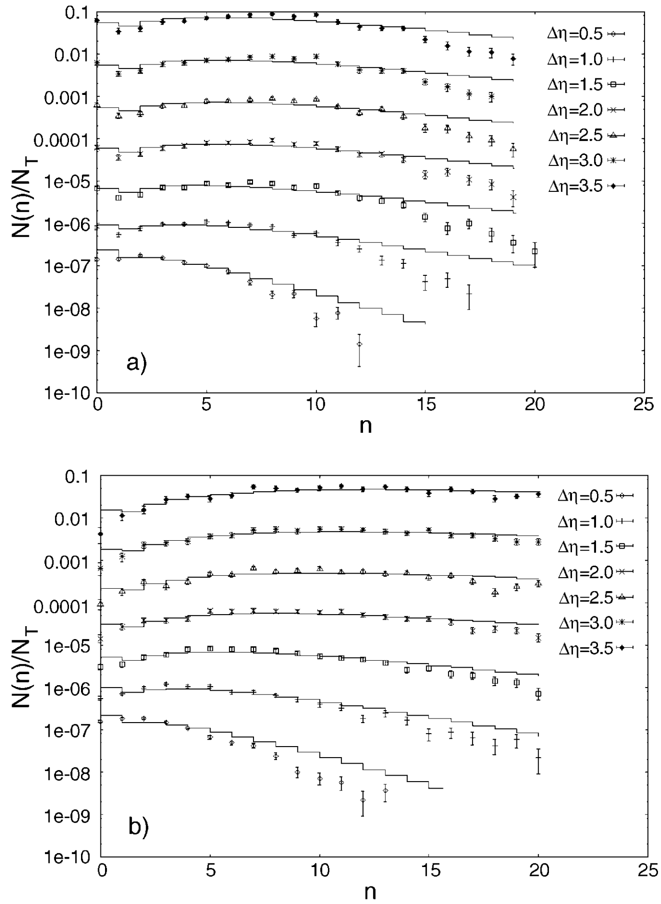

Fig. 2. Normalized multiplicity distribution, $(N(n)/N_{\mathrm{T}}$, where $N(n)$ is the number of shower particles in n-th bin and N_{T} is the total number of events) for different rapidity windows of span $\Delta\eta = 0.5$ to 3.5, a) forward hemisphere, b) backward hemisphere. Only the p-AgBr interactions are shown for clarity.

sidered N_{h} values, which are given in table 1. It can be observed that the value of average clan size $\overline{n_{\mathrm{c}}}$ remains between 1 and 2 for all the cases (even for p-N and p-nucleus interactions), inspite of variation in $\overline{n}$ (average multiplicity) with rapidity windows. This implies that even if total number of final particles increases, only average number of clans ($\overline{N}$) increases and average number of particles per clan remains nearly the same.

The clan parameters $\overline{n}$, $1/k$, $\overline{N}$ and $\overline{n_{\mathrm{c}}}$ have also been determined in forward and backward hemispheres for proton-nucleus interactions, and have been compared with those at 200 [3] and 360 [24] GeV as shown in table 2. It is seen that the average number of clans $\overline{N}$ remains unchanged with respect to primary energy as well as in forward and backward regions. The values of the average clan size $\overline{n_{\mathrm{c}}}$ are higher in the backward as compared to forward hemisphere, which could be due to higher value of $\overline{n}$ in the former in comparison to the latter hemisphere. The higher value of $\overline{n}$ in the backward hemisphere compared to that in the forward hemisphere could be due to multi-nucleon collisions in the former region.

Charged-particle multiplicity distributions have been separately analyzed in the forward and backward hemispheres. Figure 2 shows the corresponding distributions for different rapidity windows of widths $\Delta\eta = 0.5$ to 3.5. The solid line shows the NBD fit to experimental values. For purposes of clarity, the distribution for the widest width (3.5) is shown on the ordinary scale and each preceding distribution is scaled down by a factor of 10. For the purposes of present analysis, we define that a particle belongs to the forward (backward) hemisphere when its laboratory rapidity η_{Lab} is > 3.77 (< 3.77). The value $\eta_{\mathrm{Lab}} = 3.77$ corresponds to a center-of-mass rapidity of zero. We have considered seven rapidity intervals of width $\Delta\eta$, ranging from 0.5 to 3.5 units, all of them extending from the central value $\eta_{\mathrm{Lab}} = 3.77$ to the right (left), corresponding to forward (backward) hemisphere. The value $\Delta\eta = 3.5$ practically corresponds to the full phase space in forward or backward hemisphere. The dependence of

Table 3. Parameters of negative binomial distributions, for different rapidity windows $\Delta\eta$; a) p-p forward hemisphere; b) p-p backward hemisphere; c) p-CNO forward hemisphere; d) p-CNO backward hemisphere; e) p-AgBr forward hemisphere; f) p-AgBr backward hemisphere.

$\Delta\eta$		$\overline{n}$	$1/k$	$\overline{N}$	$\overline{n_{\mathrm{c}}}$
0.5	a)	2.80 ± 0.13	0.498 ± 0.02	1.75 ± 0.08	1.60 ± 0.07
	b)	2.78 ± 0.14	0.500 ± 0.02	1.74 ± 0.09	1.60 ± 0.08
	c)	2.82 ± 0.10	0.493 ± 0.02	1.77 ± 0.07	1.60 ± 0.06
	d)	3.09 ± 0.12	0.500 ± 0.02	1.87 ± 0.07	1.65 ± 0.06
	e)	3.81 ± 0.11	0.495 ± 0.01	2.14 ± 0.06	1.78 ± 0.05
	f)	4.04 ± 0.12	0.500 ± 0.01	2.21 ± 0.06	1.83 ± 0.05
1.0	a)	5.42 ± 0.23	0.500 ± 0.02	2.62 ± 0.11	2.07 ± 0.09
	b)	3.98 ± 0.18	0.500 ± 0.02	2.19 ± 0.10	1.82 ± 0.08
	c)	5.65 ± 0.19	0.500 ± 0.02	2.68 ± 0.09	2.11 ± 0.07
	d)	4.71 ± 0.17	0.498 ± 0.02	2.43 ± 0.09	1.94 ± 0.07
	e)	7.46 ± 0.21	0.493 ± 0.01	3.13 ± 0.09	2.38 ± 0.07
	f)	7.02 ± 0.19	0.500 ± 0.01	3.01 ± 0.08	2.33 ± 0.06
1.5	a)	7.42 ± 0.31	0.485 ± 0.02	3.14 ± 0.13	2.36 ± 0.10
	b)	5.01 ± 0.22	0.500 ± 0.02	2.51 ± 0.11	2.00 ± 0.09
	c)	7.54 ± 0.26	0.493 ± 0.02	3.15 ± 0.11	2.40 ± 0.08
	d)	6.23 ± 0.21	0.500 ± 0.02	2.83 ± 0.10	2.20 ± 0.08
	e)	9.37 ± 0.26	0.487 ± 0.01	3.53 ± 0.10	2.66 ± 0.07
	f)	10.71 ± 0.29	0.490 ± 0.01	3.74 ± 0.10	2.86 ± 0.08
2.0	a)	8.28 ± 0.34	0.481 ± 0.02	3.34 ± 0.14	2.48 ± 0.10
	b)	5.64 ± 0.24	0.500 ± 0.02	2.68 ± 0.12	2.22 ± 0.09
	c)	8.56 ± 0.29	0.485 ± 0.02	3.38 ± 0.11	2.53 ± 0.09
	d)	7.49 ± 0.25	0.500 ± 0.02	3.11 ± 0.11	2.41 ± 0.08
	e)	10.21 ± 0.28	0.483 ± 0.01	3.69 ± 0.10	2.77 ± 0.08
	f)	14.98 ± 0.41	0.478 ± 0.01	4.39 ± 0.12	3.41 ± 0.09
2.5	a)	8.64 ± 0.35	0.476 ± 0.02	3.43 ± 0.14	2.52 ± 0.10
	b)	6.19 ± 0.27	0.500 ± 0.02	2.82 ± 0.12	2.20 ± 0.09
	c)	9.13 ± 0.31	0.481 ± 0.02	3.50 ± 0.12	2.61 ± 0.09
	d)	8.62 ± 0.29	0.498 ± 0.02	3.35 ± 0.11	2.57 ± 0.09
	e)	10.61 ± 0.29	0.481 ± 0.01	3.76 ± 0.10	2.82 ± 0.08
	f)	18.74 ± 0.51	0.469 ± 0.01	4.86 ± 0.13	3.86 ± 0.10
3.0	a)	8.88 ± 0.36	0.481 ± 0.02	3.47 ± 0.14	2.56 ± 0.10
	b)	5.80 ± 0.25	0.498 ± 0.02	2.73 ± 0.12	2.13 ± 0.09
	c)	9.29 ± 0.31	0.483 ± 0.02	3.52 ± 0.12	2.64 ± 0.09
	d)	8.51 ± 0.29	0.495 ± 0.02	3.34 ± 0.11	2.55 ± 0.09
	e)	10.77 ± 0.30	0.481 ± 0.01	3.79 ± 0.11	2.84 ± 0.08
	f)	20.87 ± 0.56	0.467 ± 0.01	5.08 ± 0.14	4.11 ± 0.11
3.5	a)	8.93 ± 0.36	0.474 ± 0.02	3.49 ± 0.14	2.56 ± 0.10
	b)	5.95 ± 0.26	0.495 ± 0.02	2.77 ± 0.12	2.15 ± 0.09
	c)	9.32 ± 0.31	0.481 ± 0.02	3.54 ± 0.12	2.63 ± 0.09
	d)	8.83 ± 0.30	0.495 ± 0.02	3.39 ± 0.11	2.61 ± 0.09
	e)	10.77 ± 0.30	0.481 ± 0.01	3.79 ± 0.11	2.84 ± 0.08
	f)	23.23 ± 0.62	0.461 ± 0.01	5.34 ± 0.14	4.35 ± 0.12

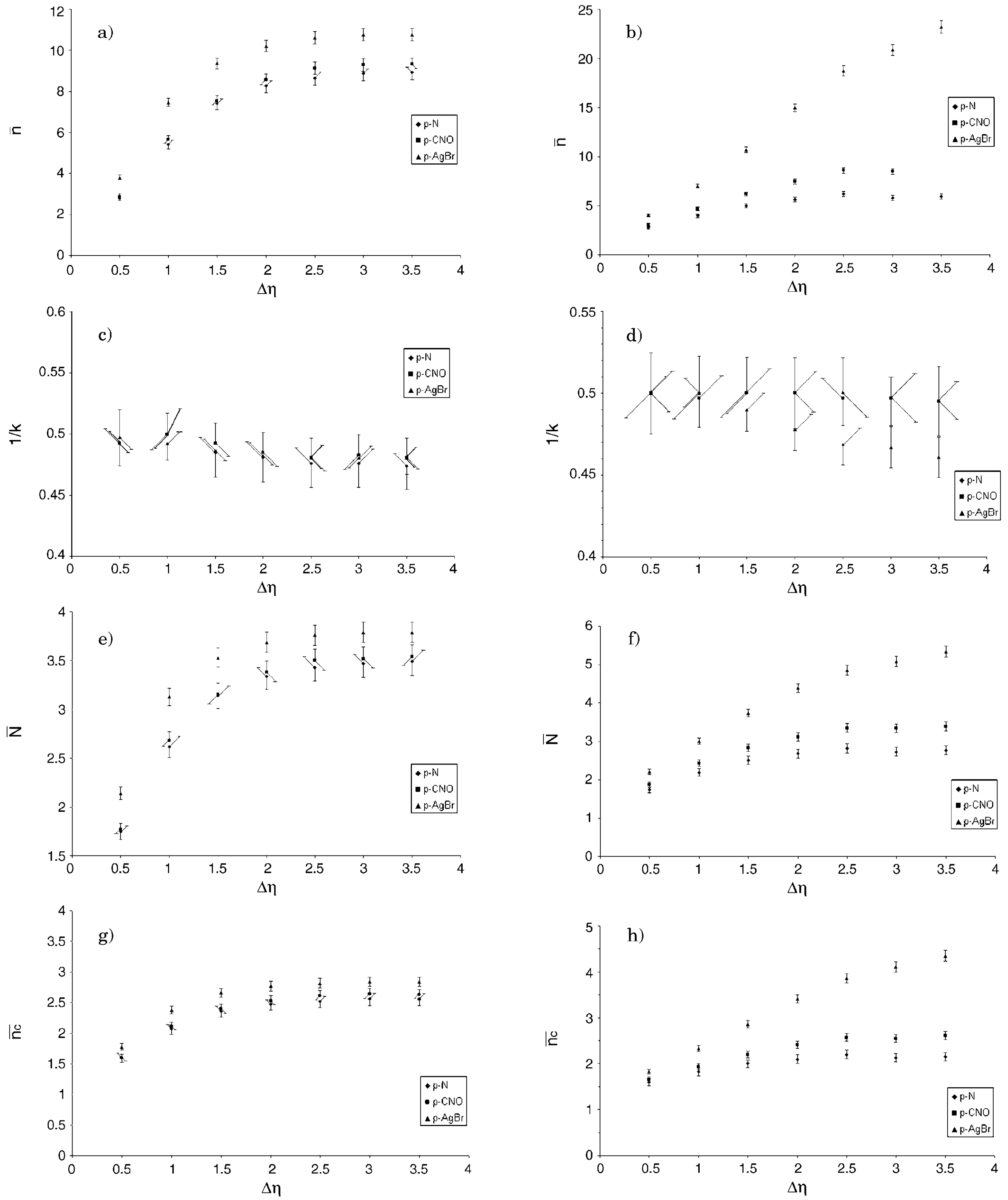

Fig. 3. Fitted values of NBD parameters as a function of rapidity windows $\Delta\eta$, for different target masses a) average multiplicity ($\overline{n}$) for the forward hemisphere, b) average multiplicity ($\overline{n}$) for the backward hemisphere, c) $1/k$ for the forward hemisphere, d) $1/k$ for the backward hemisphere, e) average clan multiplicity ($\overline{N}$) for the forward hemisphere, f) average clan multiplicity ($\overline{N}$) for the backward hemisphere, g) average clan size ($\overline{n_c}$) for the forward hemisphere, h) average clan size ($\overline{n_c}$) for the backward hemisphere. For certain values of $\Delta\eta$, two or more values are overlapping, which is shown by different error-bars at the same point.

fitted parameters, $\overline{n}$, $1/k$, $\overline{N}$ and $\overline{n_c}$ of the NBD, on the rapidity interval is shown in fig. 3, both for forward and backward hemisphere, separately for each of the targets. Table 3 gives the values of all the parameters, *i.e.*, $\overline{n}$, $1/k$, $\overline{N}$ and $\overline{n_c}$ for different rapidity windows.

The conclusions of the above study are as hereunder:

- The average multiplicity, $\overline{n}$, shows a clear target mass dependence, both in the forward and the backward hemisphere.
- In the forward hemisphere, average multiplicity, $\overline{n}$, first increases linearly with increasing width of the rapidity interval and then saturates in the region of large rapidity interval.
- In the backward hemisphere, parameter $\overline{n}$ shows a linear increase, with respect to $\Delta\eta$ window, but does not show any saturation for wider windows, in p-nucleus interactions.
- In a particular window, $1/k$ remains essentially independent of the target. However, it does not show any significant variation for different rapidity windows.
- From the variation of $\overline{n_c}$ with $\Delta\eta$ for forward hemisphere, we observe that $\overline{n_c}$ does not show a significant variation with $\Delta\eta$, and maximum $\overline{n_c}$ remains around 2.5. In addition, the clans are seen to be almost identical for p-p and p-nucleus collisions. The number $\overline{N}$ of such clans increases with the rapidity span $\Delta\eta$.

The above results match well with the corresponding results at 200 GeV [3] and 360 GeV [24]. Tannenbaum [25] and Tannenbaum *et al.* [26] have also obtained excellent fits of NBD with data in resticted rapidity windows for A-A collisions. In contrast to our results, they found a linear increase in the values of parameter k with $\Delta\eta$. As pointed out by Tannenbaum [25], this linear increase of k with $\Delta\eta$ indicates that the multiplicity distributions in adjacent $\Delta\eta$ intervals are statistically independent, while the constancy of k with $\Delta\eta$ intervals indicates 100% correlation. The existence of strong, short-range correlations in the present interactions is also supported from our earlier work [27].

We are grateful to the Fermi National Accelerator Laboratory, Illinois, for exposure facilities at the Tevatron and to Dr. Ray Stefanski for help during exposure of the emulsion stack. We would like to thank Dr. R. Wilkes for processing facilities. KR and SC would like to thank the Council for Scientific and Industrial Research, New Delhi, for financial support. Authors would like to thank Mr. Ashish Kumar for valuable discussions.

References

1. G.J. Alner *et al.*, Phys. Lett. B **160**, 193 (1985).
2. G.J. Alner *et al.*, Phys. Lett. B **160**, 199 (1985).
3. F. Dengler *et al.*, Z. Phys. C **33**, 187 (1986).
4. A. Tucholski *et al.*, Nucl. Phys. A **493**, 597 (1989).
5. M. Derrick *et al.*, Phys. Lett. B **168**, 299 (1986).
6. M. Derrick *et al.*, Phys. Rev. D **34**, 3304 (1986).
7. M. Arneodo *et al.*, Z. Phys. C **31**, 1 (1986).
8. Cherry *et al.*, Phys. Rev. D **50**, 4272 (1994).
9. D.D. Dzhalaganiya *et al.*, Sov. J. Nucl. Phys. **51**, 882 (1990).
10. C.P. Singh *et al.*, Phys. Lett. **255**, 139 (1991).
11. A. Abduzhamilov *et al.*, Phys. Rev. D **35**, 3537 (1987).
12. R. Ammar *et al.*, Phys. Lett. B **178**, 124 (1986).
13. E.A. De Wolf, Acta Phys. Pol. B **21**, 611 (1990).
14. A.K. Chaudhuri, Phys. Rev. D **45**, 4057 (1992).
15. A. Ballestro, B. Carazza, Z. Phys. C **50**, 61 (1991).
16. P. Carruthers, C.C. Shih, Int. J. Mod. Phys. A **5**, 1447 (1987). Details of the various distributions are given in the above reference.
17. A. Giovannini, L. VanHove, Z. Phys. C **30**, 391 (1986).
18. A. Giovannini, L. VanHove, Acta Phys. Pol. B **19**, 931 (1989).
19. R. Ugoccioni *et al.*, *Clan structure in Rapidity Intervals*, hep-ph/9511226.
20. R. Ugoccioni *et al.*, *Multiplicity Distributions*, in *24th International Symposium on Multiparticle Dynamics, Vietri sul Mare, Italy*, edited by Giovannini A., Lupia S., Ugoccioni R. (World Scientific, Singapore, 1995) p. 384.
21. L. Van Hove, A. Giovannini, Acta Phys. Pol. B **19**, 917 (1988).
22. R.K. Shivpuri *et al.*, Phys. Rev. D **43**, 696 (1991).
23. C. Gupt *et al.*, Phys. Rev. D **26**, 2202 (1982).
24. J.L. Bailly *et al.*, Z. Phys. C **40**, 215 (1988).
25. M.J. Tannenbaum, Mod. Phys. Lett. A **9**, 89 (1994).
26. M.J. Tannenbaum *et al.*, Nucl. Phys. A **566**, 423c (1994); Phys. Rev. C **52**, 2663 (1995).
27. Namrata *et al.*, Eur. Phys. J. A **12**, 9 (2001).